# Nonlinear Diffraction Tomography—The Use of Inverse Scattering for Imaging

W.C. Chew, G.P. Otto[1], W.H. Weedon[2], J.H. Lin, C.C. Lu, Y.M. Wang[3], and M. Moghaddam[4]
Electromagnetics Laboratory
Department of Electrical and Computer Engineering
University of Illinois
Urbana, IL 61801

### Abstract

*Our recent inverse scattering work has been to derive inverse scattering theory and algorithms that can be used to process practical experimental data. The theory makes use of computation of the forward scattering solution. Therefore, an efficient forward solver is instrumental to the rapid solution of the inverse scattering problem. The advantage of the more sophisticated theory over a linear theory is that it accounts for multiple scattering effects within the scatterers which often give rise to distortions in an image. A new method to invert strong scatterers, such as metallic scatterers, is presented.*

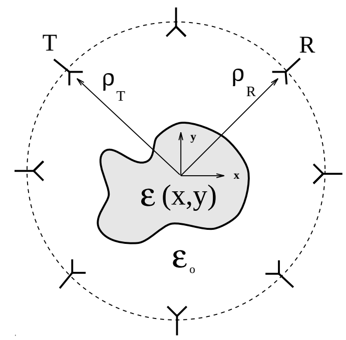


Figure 1: An inverse scattering experiment where an object is illuminated by the transmitted field, and the scattered field is measured at the receivers.

## 1 Introduction

In inverse scattering, one attempts to infer the profile of an object from measurement data collected away from the scatterer [see Figure 1]. Needless to say, this is very important for a number of sensing and remote sensing applications. For instance, it finds applications in nondestructive testing, geophysical probing, medical imaging, and target identification. In addition to obtaining the image of an object, a quantitative description of the scatterer such as its permittivity, velocity, or conductivity profile is also obtainable from an inverse scattering experiment and can be an extremely valuable diagnostic information.

Most imaging modalities use fields or waves to probe an object. In inverse scattering, one attempts to infer the object from the field perturbation, or the scattered field induced by the presence of the object. The inverse scattering problem is often quite difficult, especially when wave interactions are present. It is often non-unique because high spatial frequency portions of the object give rise to evanescent waves that cannot be measured. Multiple scattering causes the scattered field to be nonlinearly related to the scatterer. Many methods have been proposed in the past to solve particular classes of inverse scattering problems by making certain underlying assumptions about the object or scattering process. For example, in computed tomography (CT) a ray picture is used whereby it is assumed that waves propagate in straight lines and all diffraction and multiple scattering effects are ignored. Diffraction tomography (DT) takes into account diffraction, but ignores multiple scattering and assumes that the object contrast is small. Many methods have been proposed to solve the inverse scattering problem "exactly" for 1-D objects (objects such as layered media with one-dimensional spatial variations). However, to date none of these "exact" methods have been shown to be computationally stable for objects with multidimensional spatial variations [1].

In developing new inverse scattering methods, we

[1]Now with Thermo Trex Corp., San Diego, CA.
[2]Now with Northeastern University, Boston, MA.
[3]Now with Raton Technology Research, Raton, NM.
[4]Now with JPL, Pasadena, CA.

must keep in mind that the goal of this research is to develop new methods and ideas that will have a significant impact on technology. Therefore, we propose that new inverse scattering theories should be judged against the following criteria:

(1) Resolution of the reconstructed object.

(2) Maximum object contrast that may be inverted accurately.

(3) Size of the object that may be inverted.

(4) Speed of the algorithm.

(5) Valid for objects with multidimensional spatial variation.

(6) Robust, computationally stable implementation that can withstand the test of noisy or imperfect experimental data.

(7) Valid for practical scattering measurement geometries.

(8) Sufficiently general to apply to many wave equations and scattering phenomenon.

(9) Requires a minimal amount of *a priori* information about the object.

Hence, it is imperative to develop inverse scattering methods according to the above criteria. This is particularly true for nonlinear algorithms that are valid for high contrast objects and achieve a high resolution image. Many of the methods that have been developed satisfy criterion 5-9. However, more work is necessary in order to apply these methods to large objects. Also, the speed of the algorithms needs to be improved in order to reduce the turnaround time for diagnostic work. Ignoring criterions 4 and 9 often results in impractical inverse scattering algorithms.

## 2 Background on Inverse Scattering Theories

In general, the relationship between the scattered field and the scattering object is a nonlinear one. This nonlinearity comes from multiple scattering effects within the object [2]. However, a linear relationship can be found sometimes for certain limited cases. Hence, inverse scattering theories can roughly be categorized into linear inverse scattering theories and nonlinear inverse scattering theories.

In the linear inverse scattering theories, approximations are made such that a linear relationship is found between the measured data and the object. Then the information on the object is unraveled by solving the linear equations involved. For example, in X-ray tomography or computed tomography (CT), the attenuation of an X-ray is linearly related to an integral summation of the attenuations experienced by the X ray as it traverses a path [3]. Also, in nuclear magnetic resonance imaging (MRI), the received radio frequency (RF) signal is proportional to an integral summation of the resonating spin densities along a straight line [4]. The summation of an object function along a straight line is also known as a projection. A backprojection algorithm using the projection-slice theorem can be used to reconstruct the object function efficiently from its projections [2].

Another linear theory known as diffraction tomography (DT) takes into account diffraction effects for weak scattering. A linear relationship exists between the scattered field and the object because only single scattering is important. Either the Born or Rytov approximation [5] can be used to calculate the scattered field and consequently a Fourier transform relationship exists between the scattered field and the object function. The Fourier spectrum of the object function may be recovered using a filtered backpropagation algorithm as in [6] and the object therefore determined. DT is often used in ultrasonic imaging [7] to achieve good reconstructions when multiple scattering effects are small. However, when multiple scattering is important as is the case for objects with strong contrasts, the technique breaks down [8].

When multiple scattering effects are important, different nonlinear theories have been proposed to unravel the multiple scattering effects [9–17]. Many of these nonlinear theories have been developed for 1-D objects, but have not been verified as practical methods for multidimensional inverse scattering. Of particular interest is the work of Newton [12–13] who generalized the Gelfand-Levitan-Marchenko integral equation [2,17] to multidimensions. However, this method has never been numerically implemented successfully. In [11], a ray tracing method is used for the forward problem solver, but such a method is targeted for high-frequency applications.

The only general nonlinear inverse scattering theory valid for higher dimensions that has been verified to date involves numerical methods. These numerical methods are usually iterative, and a forward scattering solver is needed in each iteration [18–27]. A review of our contributions [28–40] to these algorithms will be given in the following section.

# 3 Nonlinear Inverse Scattering Methods

## 3.1 Born and Distorted Born Iterative Methods

The Born-iterative method (BIM) and distorted-Born-iterative method (DBIM) have been proposed and verified as methods of solving the nonlinear inverse scattering problem for dielectric scatterers [28–35]. A basic scalar wave equation that appears in 2-D electromagnetic scattering from a line source and also acoustic scattering is

$$\left[\nabla^2 + k^2(\mathbf{r})\right] \phi(\mathbf{r}) = S(\mathbf{r}) \tag{1}$$

where $S(\mathbf{r})$ is a radiating source and $\phi(\mathbf{r})$ represents the total field. An integral equation for the total field may be derived as [2]

$$\phi(\mathbf{r}) = \phi_{inc}(\mathbf{r}) + \int d\mathbf{r}' g_b(\mathbf{r}, \mathbf{r}') O(\mathbf{r}') \phi(\mathbf{r}'), \tag{2}$$

where $\phi_{inc}(\mathbf{r})$ is the incident field, $O(\mathbf{r}) = k^2(\mathbf{r}) - k_b^2(\mathbf{r})$ is the object function to be reconstructed and $g_b(\mathbf{r}, \mathbf{r}')$ is the background Green's function. The background Green's function is a solution to

$$\left(\nabla^2 + k_b^2(\mathbf{r})\right) g_b(\mathbf{r}, \mathbf{r}') = -\delta(\mathbf{r} - \mathbf{r}'), \tag{3}$$

for an arbitrary assumed profile $k_b(\mathbf{r})$.

In the Born iterative method [30], $k_b$ is assumed to be that of a homogeneous medium so that it is independent of $\mathbf{r}$ whence $g_b(\mathbf{r}, \mathbf{r}')$ is known in closed form. The internal field $\phi(\mathbf{r}')$ inside the integral of Eq. (2) is initially set to the incident field $\phi_{inc}(\mathbf{r})$ and the object $O(\mathbf{r})$ solved numerically as a linear inverse problem. This value of $O(\mathbf{r})$ is not exact because of the errors in the estimate of $\phi(\mathbf{r})$. However, $O(\mathbf{r})$ can be used to provide a new estimate the internal field $\phi(\mathbf{r}')$ in the integral of Eq. (2) and the process is repeated iteratively until a convergent solution is obtained [see Figure 2].

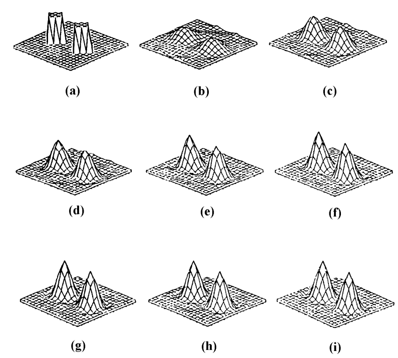

Figure 2: Inverse scattering reconstruction of two objects using the Born iterative method. (a) is the actual profile, and (i) is the solution after several iterations.

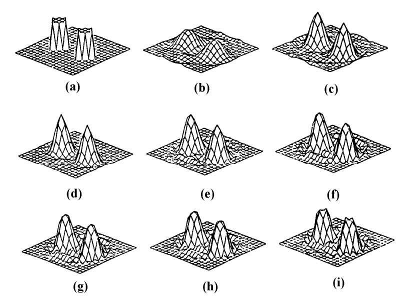

Figure 3: Inverse scattering reconstruction of two objects using the distorted Born iterative method. (a) is the actual profile, and (i) is the solution after several iterations.

In the distorted Born iterative method [28,31], the background medium $k_b(\mathbf{r})$ is not constrained to be homogeneous and is updated at each iteration. The added difficulty now is that $g_b(\mathbf{r}, \mathbf{r}')$ is no longer available in closed form and must be sought via a numerical method. However, DBIM can be shown to have second-order convergence as opposed to BIM's first-order convergence and hence is usually better for objects with large contrast. On the other hand, BIM seems to be more robust than DBIM when noise contamination is present [31]. Nevertheless, a convergent solution can be achieved [see Figure 3].

Both BIM and DBIM have been implemented for both CW and transient excitations [30–35]. Many fast forward scattering algorithm have been developed [41–46]. For the CW case, the recursive-aggregate-T-matrix-algorithm (RATMA) is used for the fast forward scattering solver [34,41–45] as well as a CG-FFT method [47,48]. Recently, such a method has been used for the inversion of well-logging data [49–51]. For the transient case, a finite-difference-time-domain (FDTD) algorithm is used as the forward solver [52]. In addition, the above algorithms have been implemented for limited-angle inverse scattering applications like subsurface probing, well-to-well tomography, etc [32,33,35]. In the limited angle reconstructions, a boosting procedure is found to greatly improve the solution [32].

## 3.2 The Local Shape Function Method

Recently, we have developed a new inverse scattering method known as the local-shape-function (LSF) method [36–39] to invert strong metallic scatterers.

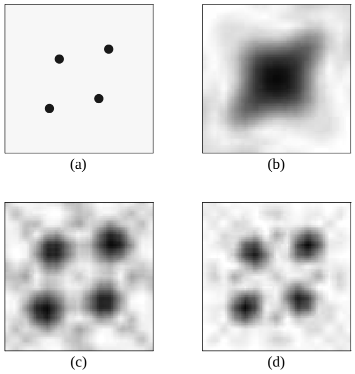


Figure 4: Image of four metal cylinders having diameter 0.1 $\lambda_{min}$: (a) true object (b) monochromatic diffraction tomography image (c) monochromatic LSF reconstruction after 11 iterations. The peak value is 0.237 (d) multifrequency LSF reconstruction after 14 iterations. The peak value is 0.454.

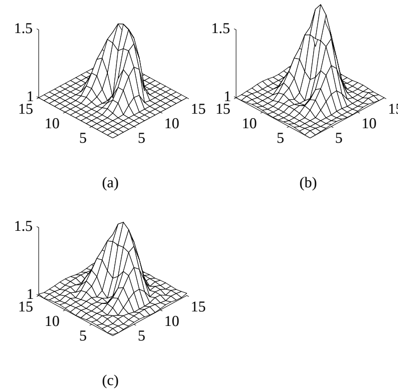


Figure 5: Reconstruction of dielectric profiles using scattered field from $H_z$ polarized waves. (a) is the actual profile, (b) is the profile reconstructed using DBIM, (c) is the profile reconstructed using LSF method.

This technique maps a scatterer with infinite conductivity into a problem with a scatterer described by a binary function which ranges between 0 and 1. By so doing, the extremely nonlinear problem of scattering by a metallic scatterer is mapped into another space where the problem is more linear, but still nonlinear. Eventually, it allows us to iteratively reconstruct metallic scatterers where the application of BIM or DBIM would converge extremely slowly or not at all.

Although we have developed LSF theory that applies to both CW and transient excitation, the LSF algorithm is more simply derived in the frequency domain. First, the scattering region is discretized by dividing the scattering volume $V$ into $N$ regions occupying volumes $V_i$, $\quad i = 1, \ldots, N$. Then, a binary shape function $\gamma_i$ is assigned to each volume $V_i$ depending on whether the individual volume contains a metallic scatterer. If $\mathcal{M}$ represents the total volume occupied by metallic scatterers, then we have

$$\gamma_i = \begin{cases} 1, & V_i \cap \mathcal{M} \neq 0, \\ 0, & V_i \cap \mathcal{M} = 0. \end{cases} \tag{4}$$

The total field may be expanded in cylindrical harmonics and written as [2, p. 465]

$$\phi(\mathbf{r}) = \Re g\ \psi^t(k_o, \mathbf{r}) \cdot \mathbf{e}_o + \sum_{i=1}^{N} \psi^t(k_o, \mathbf{r}_i) \cdot\ \mathbf{a}_i. \tag{5}$$

where the second term on the right-hand side is the scattered field, and $\psi^t(k_o, \mathbf{r}_i)$ is a vector containing the outgoing-wave cylindrical harmonics representing the field emanating from the $i-$th scatterer. The first term on the right-hand side of (5) is the incident field expanded in terms of standing wave cylindrical harmonics represented by the elements of $\Re g\ \psi^t$. Enforcing multiple scattering boundary conditions on each subscatterer $i$, we have [36,37]

$$\mathbf{a}_i = \gamma_i \cdot \bar{T}_i \cdot \left( \overline{\beta}_{i0} \cdot \mathbf{e}_o \sum_{\substack{j=1 \\ j \neq i}}^{N} \overline{\alpha}_{ij} \cdot \mathbf{a}_j \right), \quad i = 1, 2, \ldots N \tag{6}$$

where $\bar{T}_i$ is the T-matrix for the isolated subscatterer $i$ and $\overline{\alpha}_{ij}$ and $\overline{\beta}_{i0}$ are translation matrices [2]. Equation (6) may be written as

$$\tilde{\mathbf{a}} = \left[ \overline{\mathcal{D}}(\tilde{\gamma}) \cdot \overline{\mathbf{A}} + \overline{\mathbf{I}} \right]^{-1} \cdot \overline{\mathcal{D}}(\tilde{\gamma}) \cdot \overline{\mathbf{B}} \cdot \mathbf{e}_o \tag{7}$$

where $\overline{\mathbf{A}}$ and $\overline{\mathbf{B}}$ are known matrices and $\overline{\mathcal{D}}(\tilde{\gamma})$ converts the vector $\gamma$ into a diagonal matrix.

Equation (7) is important because $\mathbf{a}_i$ expresses the amplitude of the scattered field emitted from the $i$-th scatterer including multiple scattering from the other scatterers occupying volumes $V_j$, $\quad j \neq i$. For the inverse problem, we assume that $\tilde{\gamma}$ is a continuous variable, and linearize the problem at iteration $k+1$ such that

$$\begin{aligned} \overline{\phi}^{scat}(\mathbf{r}) &= \sum_{i=1}^{N} \overline{\psi}^t(k_o, \mathbf{r}_i) \cdot\ \mathbf{a}_{i,k+1} = \overline{\mathbf{\Psi}}^t \cdot \tilde{\mathbf{a}}_{k+1} \\ &\approx \overline{\mathbf{\Psi}}^t \cdot \tilde{\mathbf{a}}_k + \overline{\mathbf{G}}_k \cdot (\tilde{\gamma}_{k+1} - \tilde{\gamma}_k). \end{aligned} \tag{8}$$

In the above, $\overline{\phi}^{scat}(\mathbf{r})$ is a column vector containing the measured values of the scattered field, the sec-

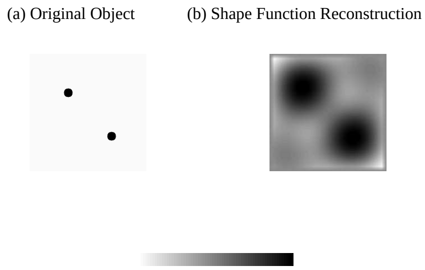


Figure 6: Reconstruction of metallic scatterers with time-domain data using the LSF method.

ond term in Equation (5), at different receiver locations, and similarly, $\overline{\psi}^t(k_o, \mathbf{r}_i)$ contains the values of $\psi^t(k_o, \mathbf{r}_i)$ at different receiver locations. Furthermore, $\overline{\Psi}^t$ is an $M \times N$ matrix where $M$ is the number of receiver locations, and $\overline{\mathbf{G}}_k$ is the Frèchet derivative with respect to $\tilde{\gamma}_k$ of the scattered field. Using a perturbation expansion of Equation (7), the Frèchet derivative may be expressed as

$$\begin{aligned} \overline{\mathbf{G}}_k = \overline{\psi}^t \cdot \left[\overline{\mathcal{D}}(\tilde{\gamma}_k) \cdot \overline{\mathbf{A}} + \overline{\mathbf{I}}\right]^{-1} \\ \cdot \overline{\mathcal{D}}\left(\left[\overline{\mathbf{A}} \cdot \overline{\mathcal{D}}(\tilde{\gamma}_k) + \overline{\mathbf{I}}\right]^{-1} \cdot \overline{\mathbf{B}} \cdot \mathbf{e}_o\right). \end{aligned} \tag{9}$$

The above represents the gradient as a cascade of one propagator that maps the incident field into the object space and a second propagator that maps the object field back out to the receivers. Hence, the $N$-dimensional gradient may be implemented with only two calls to a forward scattering solver.

Figure 4 shows the reconstruction of a typical metallic scatterer using the local shape function method on simulated data. Some experimental results using the local shape function method for real data are described in the section on "Work With Experimental Data."

We have also studied the use of the local-shape function method for the reconstruction of dielectric profile for the highly nonlinear inverse problem of $H_z$-wave scattering [38]. The $H_z$-wave scattering problem maps into the variable density problem for acoustic waves. Hence, this method can also be potentially applied to improve the reconstruction of ultrasonic images. Figure 5 shows the reconstruction of the dielectric profile using scattered field from $H_z$-polarized waves. Compared to DBIM, the LSF method yields a convergent solution for a much larger range of contrasts.

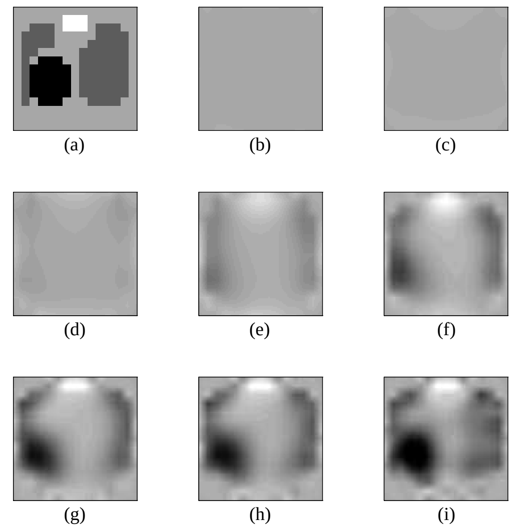


Figure 7: Inversion of an inhomogeneous conductivty profile to simulate the 2-D cross-section of a human chest. The background conductivity is 0.04 S/m. The bone, lungs, and heart are 0.006 S/m, 0.076 S/m, and 0.17 S/m respectively. The subject diameter is 0.22 m and the electrode radius is 0.15 m. (a) True profile. (b)-(i) Results of first through eighth iterations.

The method is also being extended to the processing of time-domain data in time-domain inverse scattering [39]. A sample result is shown in Figure 6.

Recently, we have also extended the use of a method similar to the local-shape function method for electrical impedance tomography. Figure 7 shows the use of the local-shape function T-matrix method to a reconstruction in electrical impedance tomography [53].

### 3.3 Observation of Super-resolution

Super-resolution, that is resolution beyond the Rayleigh criterion of 0.5 wavelengths ($\lambda$) has been observed for the BIM and DBIM algorithms [30,31,33,35]. When either the BIM or DBIM method is used to process the scattering data from two closely spaced point objects, the objects may be resolved when they are spaced by as little as 0.1 $\lambda$ apart [33–35]. The LSF at present is able to distinguish point objects (metallic scatterers) separated by 0.42 $\lambda$. However, the image resulting from LSF is still much sharper than that resulting from diffraction tomography and significantly reduces the number of "phantom" reconstructions [37].

In Figure 8, some typical image reconstructions demonstrating this super-resolution are shown. The

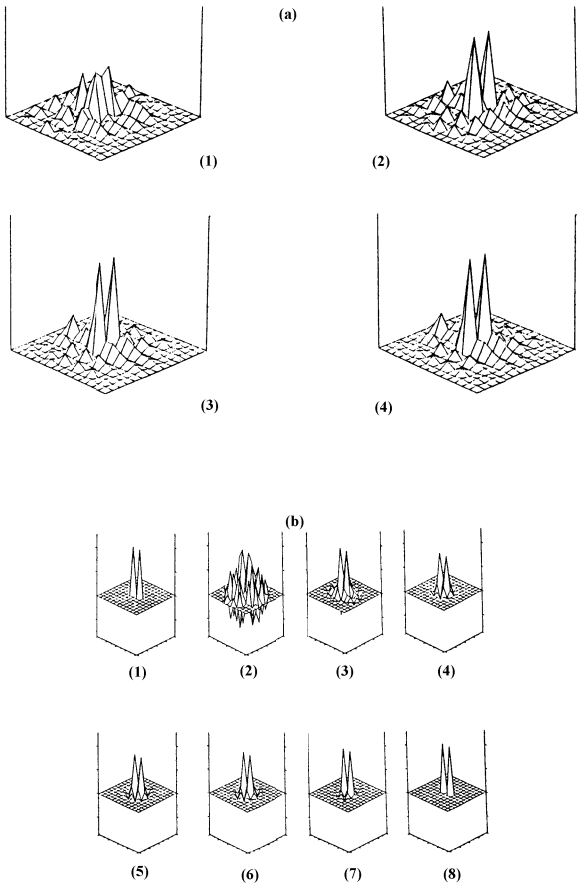


Figure 8: (a) Horizontal resolution of two point objects placed 0.1 wavelength apart with contrast of 2:1. (1)-(4) Results of second, fourth, sixth, and eighth iterations, using time domain Born iterative method. (b) Reconstruction of two single-pixel pulses separated by one pixel with the same contrast using CW distorted Born iterative method at 100 MHz. The diameter of the reconstructed area is 3.0 meters. (1) Original distribution. (2) Result of the first-order approximation. (3)-(7) Results from the second iteration to the seventh iteration. (8) Final convergent solution after twenty iterations.

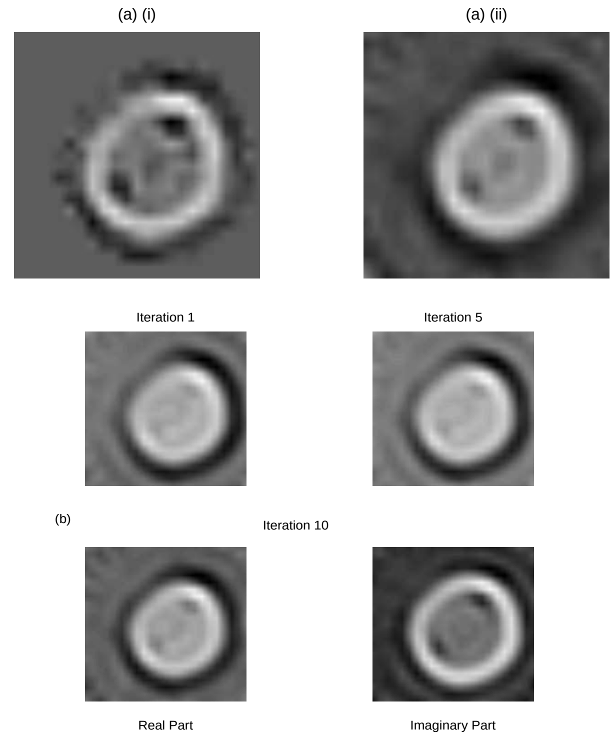


Figure 9: (a) Reconstructed microwave image of a human arm at 2.5 GHz, with 64 transmitters and 33 receivers using (i) the fast recursive algorithm (RATMA), and (ii) the CG-FFT algorithm. The arm is immersed in water. Its shape and bones are clearly visible. (b) Reconstruction of the microwave image at different iterations of the distorted Born iterative method. The first iteration corresponds to a linear theory, and hence, resembles the solution from diffraction tomography. The imaginary part of the reconstruction is shown as well.

receivers are placed about ten wavelengths away so that the evanescent spectrum is negligible.

### 3.4 Work With Experimental Data

All of the inverse scattering methods described thus far, the BIM, DBIM and LSF have been used to process real data. The CW implementation of the DBIM was recently used to process microwave scattering data collected by a group in Barcelona, Spain [54,48]. Previously, diffraction tomography was used to process the data resulting in a poor resolution image due to the high contrasts present in the human body. Using the DBIM, the processed image was significantly improved and the result is shown in Figure 9.

The local shape function method in time domain

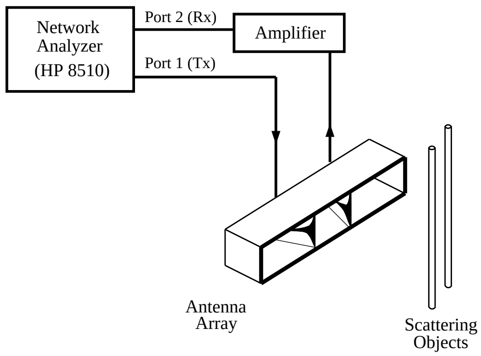


Figure 10: Sketch of a prototype step-frequency radar (SFR) broadband inverse scattering measurement system constructed at the University of Illinois.

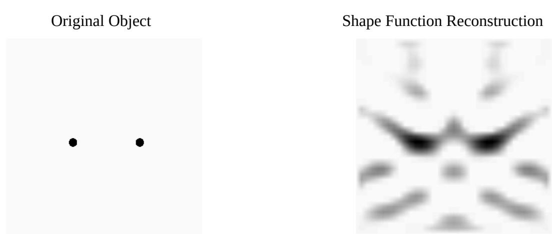


Figure 11: Original object and shape function reconstruction from experimental data of two metallic cyinders of diameter 0.4 cm aligned horizontally with separation 3.2 cm. The experimental data was collected with the prototype step-frequency radar shown in the previous figure.

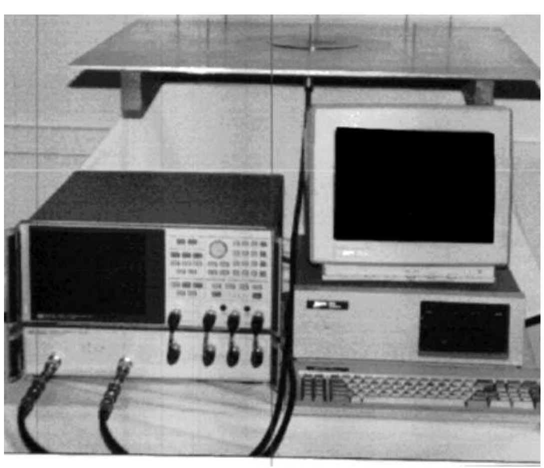

Figure 12: Prototype microwave monopole imaging array developed at the University of Illinois.

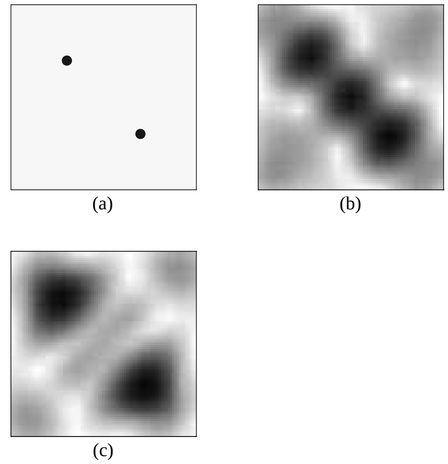


Figure 13: Measured data image reconstructions of two metal cylinders having diameter 1.9 cm and centers separated by 18.0 cm at 1 GHz. The grid spacing is 2.14 cm: (a) True objects. (b) Diffraction tomography image (c) Reconstruction after fifteen LSF iterations. The peak value is 0.083.

[40] has also been used to process experimental data collect by a step frequency radar (SFR) developed at the University of Illinois. The SFR is used for nondestructive evaluation (NDE) purposes to locate and identify cracks and voids in concrete structures, as well as metallic reinforcement bars (rebars) and utility pipes. The SFR apparatus is shown in Figure 10. Using the LSF algorithm in the time domain, reconstructions were obtained with higher quality than that attainable previously using a method similar to DT involving straight backpropagation (see Figure 11). However, due to the primitive measurement apparatus the reconstructions do not represent the capabilities of the inverse algorithm. A new system needs to be designed and built to achieve more sensitive measurements with more data diversity in order to realize the capability demonstrated using simulated data.

The LSF method in the frequency domain was also demonstrated experimentally at the Electromagnetics Laboratory, University of Illinois at Urbana-Champaign using the apparatus shown in Figure 12. This first-generation system employed 8 monopole antennas located symmetrically around a circle of radius 0.3 meter and mounted on a square ground plane with sides 1 meter in length. A major problem with the apparatus was the scattering effect caused by the monopole elements that were not active and also effects due to the finite ground plane. Nevertheless, some fairly good results were achieved and are demon-

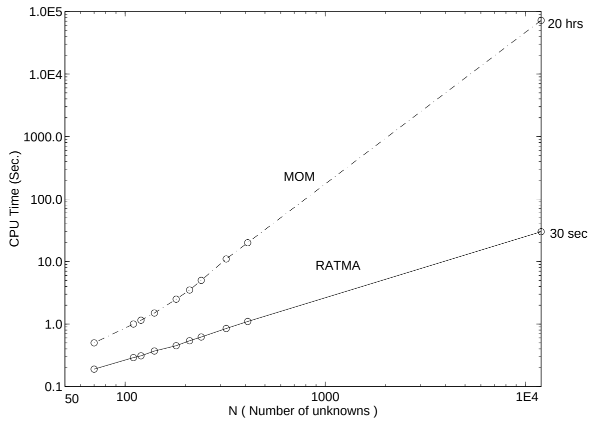


Figure 14: Comparison of the growth of CPU time of RATMA (recursive aggregate T matrix algorithm) (black dots) versus method of moments (white dots) with Gaussian elimination for a scatterer with different numbers of unknowns. For a scatterer with 12,000 unknowns, MOM can take about 20 hours while RATMA would take about 30 seconds. The 12,000 unknown point for the method of moments is extrapolated.

strated in Figure 13.

### 3.5 Fast Forward Solvers

In all the nonlinear inverse scattering theories which are multidimensional, practical and can be applied to pragmatic problems, a forward scattering solver is required. Often, the forward solver is the computational bottleneck in the inverse scattering algorithm. Hence, if a high speed forward solver is used, it will greatly expedite the inverse scattering algorithm. We have made significant advances in the development of fast algorithms for forward scattering theory that can be applied to inverse scattering [41–46]. Figure 14 shows the growth of the CPU time of using RATMA and the method of moments [55].

### 3.6 Conclusions

A review of the work on inverse scattering for imaging application is given. It is seen that much work is still needed in this area to yield a matured technology. Progress in the area of microwave inverse scattering will have a significant technological impact. It will allow inverse scattering theory to be more easily applied to medical imaging, nondestructive testing, geophysical sensing, target identification, etc. Further research of inverse scattering theory will allow the expansion of the electromagnetic and acoustic spectrum that may be used for imaging and artificial sight, and will allow for the development of better imaging methods. For example, in biomedical imaging where accuracy is extremely important, these methods will remove distortions of reconstructed images inherent in existing algorithms that account for single wave scattering phenomenon only.

In geophysics, this will better enable the detection of hydrocarbon and mineral resources using seismic, electromagnetic, and acoustic waves. In nondestructive testing, it will aid in eddy current imaging and subsurface interface radar imaging systems that can be used for the detection of fractures in structures, constructed works, location of reinforcement bars, etc. In remote sensing, it will help in the interpretation of remotely sensed data from satellites and space shuttles. In target identification, it could improve on existing technologies in this field. The list of technologies on which inverse scattering theory could have an impact is long, and the above list is incomplete.

## Acknowledgements

This work was supported by the Office of Naval Research under grant N00014-89-J1286, and the National Science Foundation under grant NSF ECS 92-24466. The computer time was provided by the National Center for Supercomputing Applications (NCSA) at the University of Illinois at Urbana-Champaign.

The authors like to thank A. Broquetas and J.J. Mallorqui of Universitat Politècnica de Catalunya, Barcelona, Spain for making their experimental data available to us, and also to J.-Ch. Bolomey, Ch. Pichot and their coworkers for helps rendered with the Barcelona data.

## References

[1] M. Cheney and G. Kristensson, "Three dimensional inverse scattering: layer-stripping formulae and ill-posedness results," *Inverse Problem*, 4, pp. 625–642, 1988.

[2] W. C. Chew, *Waves and Fields in Inhomogeneous Media*: Van Nostrand Reinhold, 1990.

[3] A. C. Kak, "Computerized tomography with X-ray, emission, and ultrasound sources," *Proc. IEEE*, vol. 67, no. 9, pp. 1245–1272, 1979.

[4] P. C. Lauterbur, "Medical imaging by nuclear magnetic resonance zeugmatography," *IEEE Trans. Nucl. Sci.*, vol. 27, no. 2, pp. 2808–2811, 1973.

[5] M. Born and E. Wolf, *Principles of Optics*, Pergamon Press, New York, First Edition, 1959, Sixth Edition, 1980.

[6] A. J. Devaney, "A filtered backpropagation algorithm for diffraction tomography," *Ultrasonic Imaging*, vol. 4, pp. 336– 360, 1982.

[7] M. Slaney, A. C. Kak, and L. E. Larsen, "Limitations of imaging with first-order diffraction tomography," *IEEE Trans. Microwave Theory Tech.*, vol. MTT–32, pp. 860–874, 1984.

[8] H. Lee and G. Wade, *Modern Acoustic Imaging*, IEEE Press, 1986.

[9] F. C. Lin and M. A. Fiddy, "Image estimation from scattered field data," *Int. J. Imag. Sys. Tech.*, vol. 2, pp. 76–95, 1990.

[10] E. Baysal, D. D. Kosloff, and J. W. C. Sherwood, "Reverse time migration," *Geophysics*, vol. 48, no. 11, pp. 1514–1524, 1983.

[11] J. G. Berryman, "Weighted least-square criteria for seismic traveltime tomography," *IEEE Trans. Geosci. Remote Sensing*, vol. GE–27, no. 3, pp. 302–309, 1989.

[12] R. G. Newton, "Inverse scattering II. Three dimensions," *J. Math. Phys.*, vol. 21, no. 7, pp. 1698–1715, 1980.

[13] R. G. Newton, "Inverse scattering III. Three dimensions, continued," *J. Math. Phys.*, vol. 22, no. 10, pp. 2191–2200, 1981.

[14] J. H. Rose, M. Cheney, and B. DeFacio, "The connection between time- and frequency-domain three-dimensional inverse scattering methods," *J. Math. Phys.*, vol. 25, pp. 2995–3000, 1984.

[15] D. Colton and P. Monk, "The inverse scattering problem for time harmonic acoustic waves in an inhomogeneous medium," *Quart. J. Mech. Appl. Math.,* vol. 41, pp. 97–125, 1988.

[16] T. S. Angell, R. E. Kleinman, and G. F. Roach, "An inverse transmission problem for the Helmholtz equation," *Inverse Problems,* vol. 3, pp. 149–180, 1987.

[17] T. M. Habashy and R. Mittra, "On some inverse methods in electromagnetics," *J. Electromag. Waves Appl.*, vol. 1, pp. 25–28, 1987.

[18] J. -Ch. Bolomey, Ch. Durix, and D. Lesselier, "Determination of conductivity profiles by time-domain reflectometry," *IEEE Trans. Antennas Propagat.*, vol. AP–27, pp. 244–248, 1979.

[19] S. A. Johnson and M. L. Tracy, "Inverse scattering solutions by a sinc basis, multiple source, moment method—part I: theory," *Ultrasonic Imaging*, vol. 5, pp. 361–375, 1983.

[20] S. A. Johnson and M. L. Tracy, "Inverse scattering solutions by a sinc basis, multiple source, moment method—part II: numerical evaluations," *Ultrasonic Imaging*, vol. 5, pp. 376–392, 1983.

[21] T. J. Cavicchi and W. D. O'Brien, "Numerical study of high-order diffraction tomography via the sinc basis moment method," *Ultrasonic Imaging*, vol. 11, pp. 42–74, 1989.

[22] R. E. Kleinman and P. M. van den Berg, "Nonlinearized approach to profile inversion," *Int. J. Imag. Sys. Tech.*, vol. 2, pp. 119–126, 1990.

[23] J. -Ch. Bolomey and Ch. Pichot, "Microwave tomography: from theory to practical imaging systems," *Int. J. Imag. Sys. Tech.*, vol. 2, pp. 144–156, 1990.

[24] A. Tarantola, "The seismic reflection inverse problem," in *Inverse problems of acoustic and elastic waves*, F. Santosa, Y. H. Pao, W. Symes, and C. Holland, Eds.: Soc. Industr. Appl. Math., 1984.

[25] E. Crase A. Pica, M. Noble, J. McDonald, and A. Tarantola, "Robust nonlinear waveform inversion: Application to real data," *Geophysics*, vol. 55, no. 5, pp. 527–538, 1990.

[26] P. Mora, "Nonlinear two-dimensional elastic inversion of multioffset seismic data," *Geophysics*, vol. 52, no. 9, pp. 1211–1228, 1987.

[27] N. Joachimowicz, Ch. Pichot, and J.-P. Hugonin, "Inverse scattering: An iterative numerical method for electromagnetic imaging," *IEEE Trans. Antennas Propagat.*, vol. AP–39, no. 12, pp. 1742-1752, December 1991.

[28] W. C. Chew and S. L. Chuang, "Profile inversion of a planar medium with a line source or a point source," presented at *IGARSS, IEEE*, Strasbourg, France, 1984.

[29] T. M. Habashy, W. C. Chew, and E. Y. Chow, "Simultaneous reconstruction of permittivity and conductivity profiles in a radially inhomogeneous slab," *Radio Sci.*, vol. 21, no. 4, pp. 635–645, 1986.

[30] Y. M. Wang and W. C. Chew, "An iterative solution of the two-dimensional electromagnetic inverse scattering problem," *Int. J. Imag. Sys. Tech.*, vol. 1, pp.100–108, 1989.

[31] W. C. Chew and Y. M. Wang, "Reconstruction of two-dimensional permittivity distribution using the distorted Born iterative method," *IEEE Trans. Medical Imag.*, vol. 9, no. 2, pp. 218–225, 1990.

[32] Y. M. Wang and W. C. Chew, "Limited angle inverse scattering problems and their applications for geophysical explorations," *Int. J. Imag. Sys. Tech.*, vol. 2, no. 2, pp. 96–111, 1990.

[33] M. Moghaddam and W. C. Chew, "Nonlinear two-dimensional velocity profile inversion in the time domain," *IEEE Trans. Geosci. Remote Sensing*, vol. GE–30, no. 1, pp. 147–156, Jan 1992.

[34] Y. M. Wang and W. C. Chew, "Accelerating the iterative inverse scattering algorithms by using the fast recursive operator algorithm," *Radio Sci.,* vol. 27, no. 2, pp. 109–116, March–April 1992.

[35] M. Moghaddam, W. C. Chew, and M. Oristaglio, "Comparison of the Born iterative method and Tarantola's method for an electromagnetic time-domain inverse problem," *Int. J. Imag. Sys. Tech.*, vol. 3, no. 4, pp. 318–333, 1991.

[36] W. C. Chew and G. P. Otto, "Microwave imaging of multiple metallic cylinders using shape functions," *Micro. Guided Wave Lett.*, vol. 2, no. 7, pp. 284–286, 1992.

[37] G. P. Otto and W. C. Chew, "Microwave inverse scattering—local shape function (LSF) imaging for improved resolution of strong scatterers," *IEEE Trans. Microwave Theory Tech.* vol. MTT-42, no. 1, pp. 137-141, 1994.

[38] G. P. Otto and W. C. Chew, "Inverse scattering of $H_z$ waves using local shape function imaging: A T-matrix formulation," *Int. J. Imag. Sys. Tech.*, vol. 5, pp. 22-27, 1994.

[39] W. H. Weedon and W. C. Chew, "Time-domain inverse scattering using the local shape function (LSF) method," *J. Inverse Problems*, vol. 9, pp. 551-564, 1993.

[40] W. H. Weedon and W. C. Chew, "Broadband microwave inverse scattering for nondestructive evaluation (NDE)," *Quantitative Nondestructive Evaluation Conference,* Bowdoin College, Maine, 1993.

[41] W. C. Chew, "An $N^2$ algorithm for the multiple scattering solution of $N$ scatterers," *Micro. Opt. Tech. Lett.*, vol. 2, no. 11, pp. 380–383, 1989.

[42] Y. M. Wang and W. C. Chew, "An efficient algorithm for solution of a scattering problem," *Micro. Opt. Tech. Lett.*, vol. 3, no. 3, pp. 102–106, March, 1990.

[43] W. C. Chew and Y. M. Wang, "A fast algorithm for solution of a scattering problem using a recursive aggregate tau matrix method," *Micro. Opt. Tech. Lett.*, vol. 3, no. 5, pp. 164–169, May 1990.

[44] Y. M. Wang and W. C. Chew, "Solution of large 2-D inhomogeneous scatterers for TM waves by fast recursive algorithm," *Micro. Opt. Tech. Lett.*, vol. 4, no. 3, March 1991.

[45] W. C. Chew, L. Gurel, Y. M. Wang, G. Otto, R. Wagner, and Q. H. Liu, "A generalized recursive algorithm for wave-scattering solutions in two dimensions," *IEEE Trans. Microwave Theory Tech.*, vol. MTT–40, no. 4, pp. 716–723, April 1992.

[46] W. C. Chew and C. C. Lu, "The use of Huygens' equivalence principle for solving the volume integral equation of scattering," *IEEE Trans. Antennas Propagat.*, vol. AP–41, no. 7, pp. 897-904, July 1993.

[47] D. T. Borup, S. A. Johnson, W. W. Kim, and M. J. Berggren, "Nonperturbative diffraction tomography via Gauss-Newton iteration applied to the scattering integral equation," *Ultrasonic Imaging*, vol. 14, pp. 69-85, 1992.

[48] J. H. Lin, C. C. Lu, Y. M. Wang, W. C. Chew, J. J. Mallorqui, A. Broquetas, Ch. Pichot and J.-Ch. Bolomey, "Processing microwave experimental data with the distorted Born iterative method of nonlinear inverse scattering," *IEEE Antennas and Propagation Society International Symposium Digest*-vol. 1, pp. 500-503, June 28-July 2, University of Michigan, Ann Arbor, Michigan, 1993.

[49] Q.H. Liu, "Reconstruction of two-dimensional axisymmetric inhomogeneous media," *IEEE Trans. Geosci. Remote Sens.*, vol. 31, pp. 587-594, May 1993.

[50] Q.H. Liu, "Nonlinear inversion of electrode-type resistivity measurements," *IEEE Trans. Geosci. Remote Sens.*, vol. 32, no. 3, pp. 499-507, May 1994.

[51] W.C. Chew and Q.H. Liu, "Inversion of induction tool measurements using the distorted Born iterative method and CG-FFHT," *IEEE Trans. Geosci. Remote Sens.*, vol. 32, no. 4, pp. 878-884, July 1994.

[52] A. Taflove and M. E. Brodwin, "Numerical solution of steady-state electromagnetic scattering problems using the time-dependent Maxwell's equations," *IEEE Trans. Microwave Theory Tech.*, vol. MTT–23, pp. 623–630, 1975.

[53] G.P. Otto and W.C. Chew, "Time harmonic impedance tomography using the T-matrix method," *IEEE Trans. Med. Imag.*, vol. 13, no. 3, pp. 508–516, September 1994.

[54] A. Broquetas, J. Romeu, J. M. Rius, A. R. Elias-Fuste, A. Cardama, and L. Jofre, "Cylindrical geometry: a further step in active microwave tomography," *IEEE Trans. Microwave Theory Tech.*, vol. MTT–39, no. 5, pp. 836–844, 1991.

[55] R. Harrington, *Field Computation by Moment Method.* Malabar, FL: Krieger, 1983 (First printing, 1968).